nature astronomy

Article https://doi.org/10.1038/s41550-024-02200-3

Physical properties of asteroid Dimorphos as derived from the DART impact

In the format provided by the authors and unedited

Supplementary

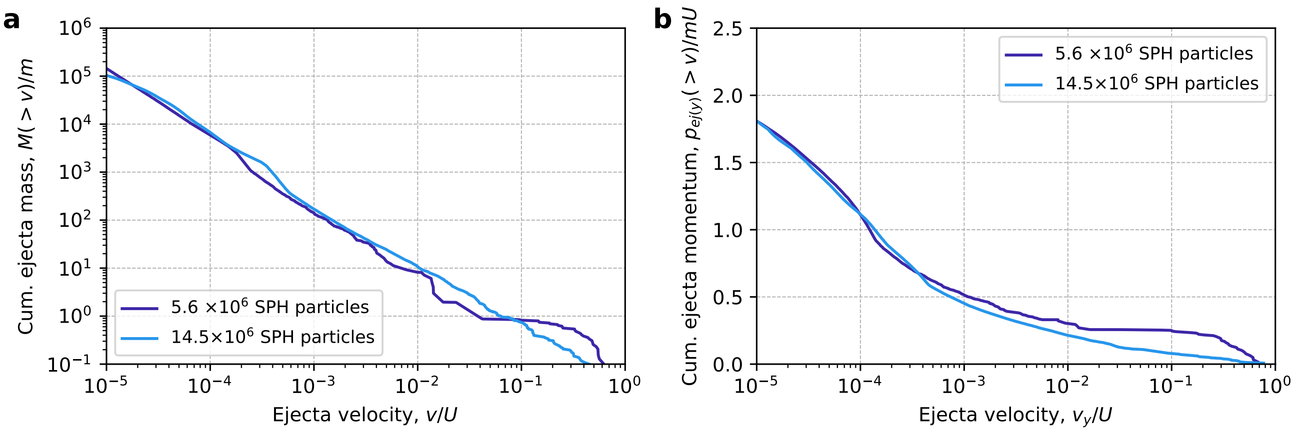

Supplementary Fig. 1: Resolution tests from an impact into rubble-pile targets ($Y_0 = 0$ Pa, $f = 0.55$, $\phi_0 = 45\%$), resolved with 5.6×10^6 and 14.5×10^6 SPH particles. (a) Normalised ejected mass at speeds greater than v, as a function of normalised ejection speed, v/U. (b) Cumulative ejected momentum as a function of normalised vertical ejection velocity (in the $-y$ direction) for impacts into targets resolved with 5.6×10^6 and 14.5×10^6 SPH particles. The data were analysed at $T = 200$ seconds after the impact.

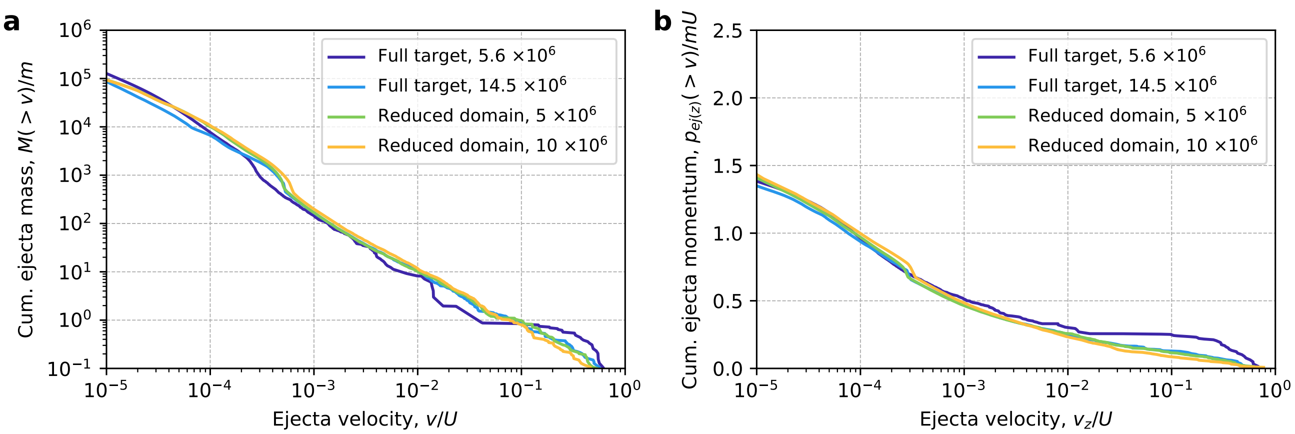

Supplementary Fig. 2: Resolution tests from an impact into rubble-pile targets ($Y_0 = 0$ Pa, $f = 0.55$, $\phi_0 = 45\%$), where the entire target was resolved with 5.6×10^6 and 14.5×10^6 SPH particles and from impacts into targets that had a reduced domain size ($\approx 15\%$ of the target in the y-direction) and was resolved by 5×10^6 and 10×10^6. a) Normalised ejected mass at speeds greater than v, as a function of normalised ejection speed, v/U. (b) Cumulative ejected momentum as a function of normalised vertical ejection velocity (in the $-y$ direction). The data were analysed at $T = 1$ second after the impact.

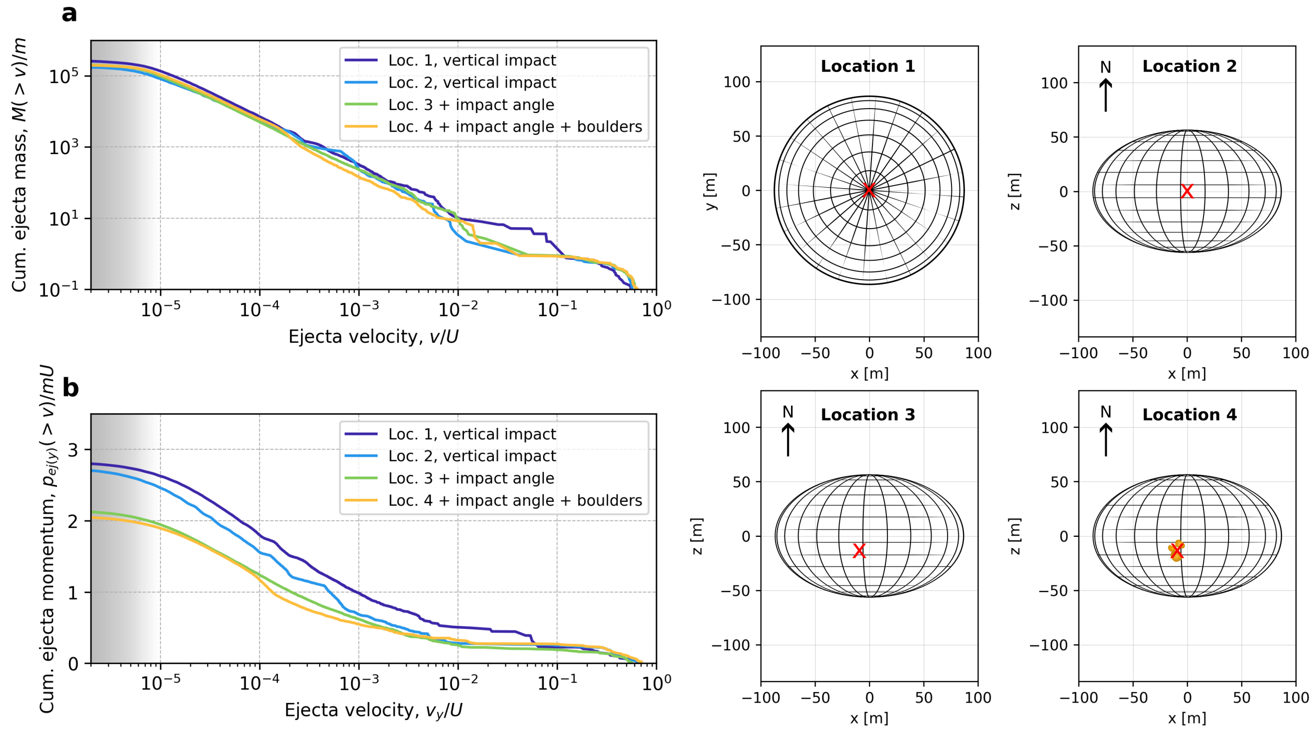

Supplementary Fig. 3: (a) Normalised ejected mass at speeds greater than v as a function of normalised ejection speed, v/U, for DART-like impacts at four different locations. (b) Cumulative ejected momentum as a function of normalised vertical ejection velocity (in the $+z$ direction for location 1 and in the $-y$ direction for locations 2–4). In all cases, the ejecta is analysed at $T \approx 30$ minutes after the impact. The shaded region shows the ejecta with velocities below the escape speed of Dimorphos, which do not contribute toward β.

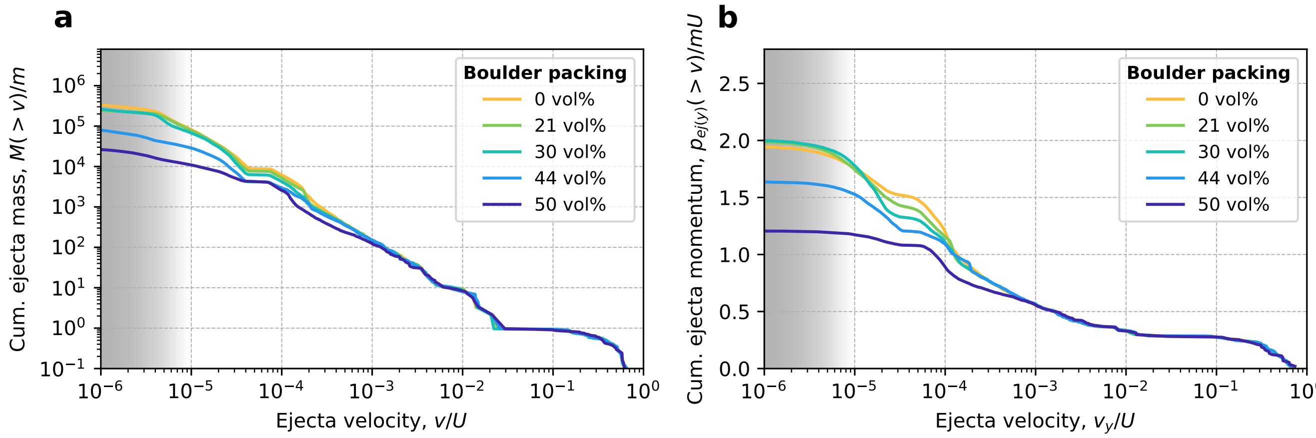

Supplementary Fig. 4: (a) Normalised ejected mass at speeds greater than v as a function of normalised ejection speed, v/U, for the DART impact into rubble-pile targets with boulder volume fractions between 0% (only the three boulders at the impact location) and 50 vol%. (b) Cumulative ejected momentum as a function of normalised vertical ejection velocity (in the $-y$ direction). In all cases, the ejecta is analysed at $T \approx 30$ minutes after the impact. The shaded region shows the ejecta with velocities below the escape speed of Dimorphos, which do not contribute toward β. The gradient is representative of the uncertainty in the escape speed calculation.

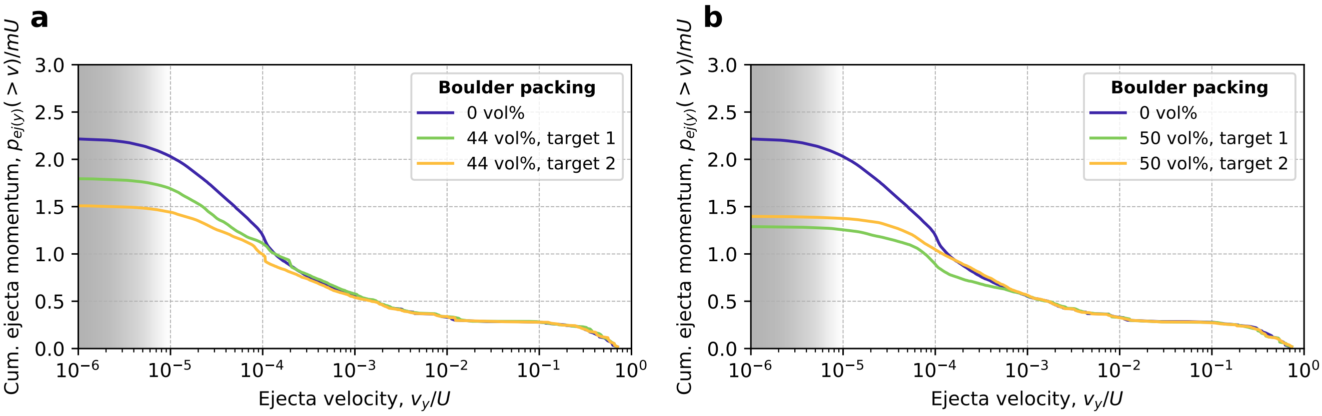

Supplementary Fig. 5: Cumulative ejected momentum as a function of normalised vertical ejection velocity (in the $-y$ direction) from impacts into (a) targets with 44 vol% boulder packing compared to a homogeneous target; (b) targets with 50 vol% boulder packing compared to a homogeneous target. In all cases, the ejecta is analysed at $T \approx 30$ minutes after the impact. The shaded region shows the ejecta with velocities below the escape speed of Dimorphos, which do not contribute toward β. The gradient is representative of the uncertainty in the escape speed calculation.

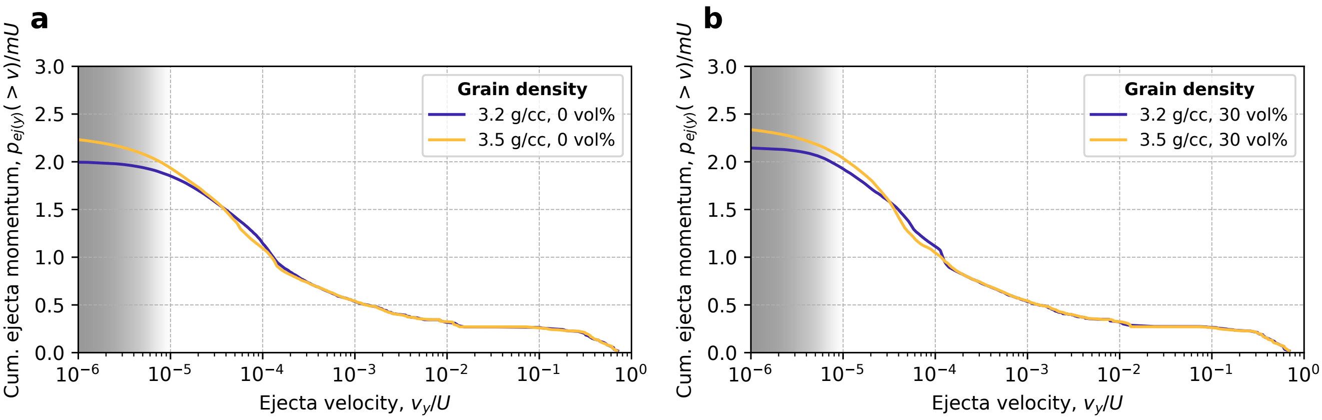

Supplementary Fig. 6: Cumulative ejected momentum as a function of normalised vertical ejection velocity (in the $-y$ direction) from impacts into (a) homogeneous targets (0 vol% occupied by boulders) and grain densities, $\rho_g = 3.2$ and 3.5 g/cc; (b) rubble-pile targets with 30 vol% occupied by boulders and $\rho_g = 3.2$ and 3.5 g/cc. The data is analysed at $T \approx 30$ minutes after the impact. The shaded region shows the ejecta with velocities below the escape speed of Dimorphos, which do not contribute toward β. The gradient is representative of the uncertainty in the escape speed calculation.

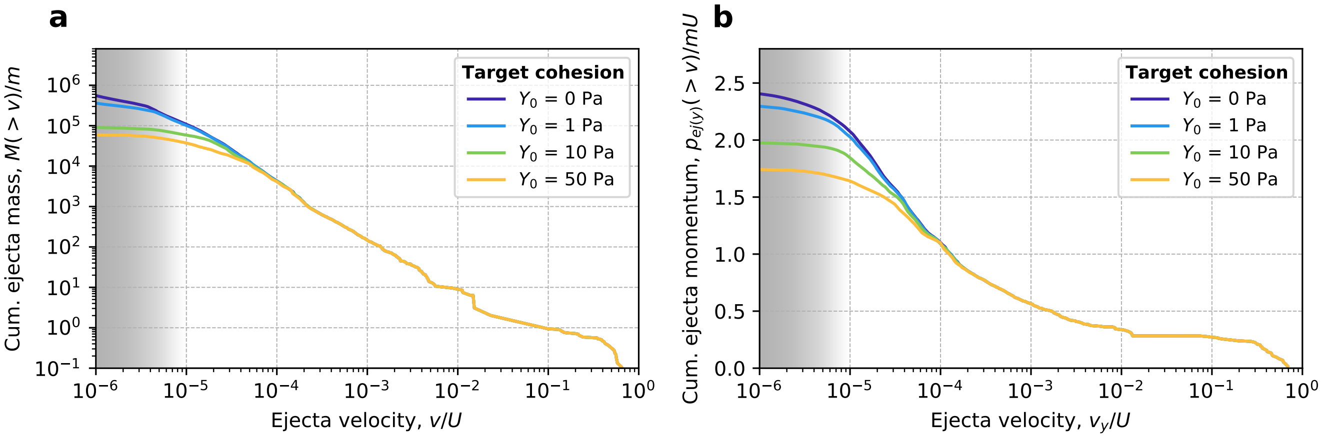

Supplementary Fig. 7: (a) Normalised ejected mass at speeds greater than v as a function of normalised ejection speed, v/U, for target matrix cohesions, Y_0, between 0 and 50 Pa. (b) Cumulative ejected momentum as a function of normalised vertical ejection velocity (in the -y direction). The shaded region shows the ejecta with velocities below the escape speed of Dimorphos, which do not contribute toward β. The gradient is representative of the uncertainty in the escape speed calculation.

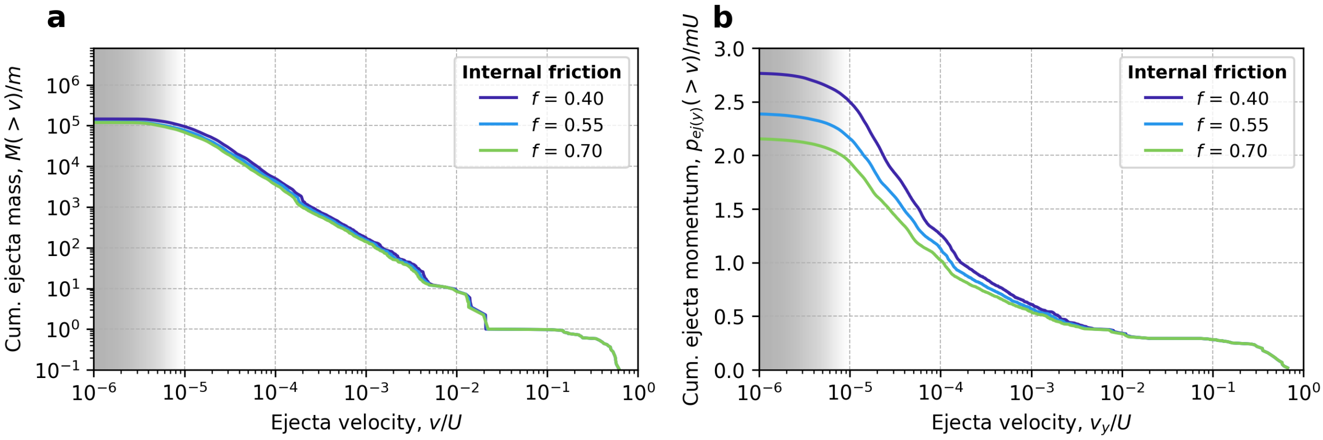

Supplementary Fig. 8: (a) Normalised ejected mass at speeds greater than v as a function of normalised ejection speed, v/U, for target matrix coefficient of internal frictions, f between 0.4 and 0.7. (b) Cumulative ejected momentum as a function of normalised vertical ejection velocity (in the -y direction). The shaded region shows the ejecta with velocities below the escape speed of Dimorphos, which do not contribute toward β. The gradient is representative of the uncertainty in the escape speed calculation.

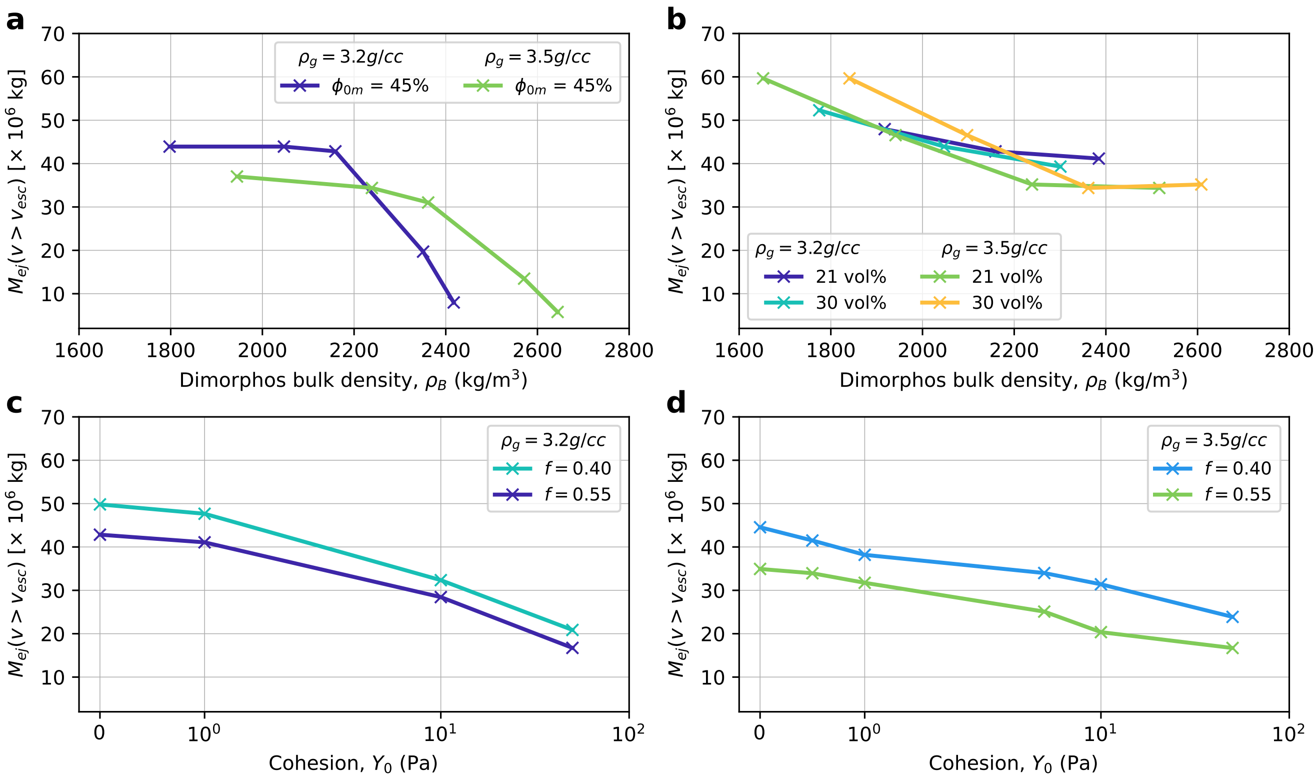

Supplementary Fig. 9: Ejecta mass from SPH simulations. (a) Ejecta mass, $M_{ej}(v > v_{esc})$, as a function of Dimorphos' bulk density, ρ_B, for Dimorphos-like targets with boulder volume fractions ranging from 0 vol% (no boulders) to 50 vol%. (b) $M_{ej}(v > v_{esc})$ as a function of bulk density, ρ_B, for Dimorphos-like targets with varying matrix porosity, between 35 and 65%. ρ_B is calculated for a fixed volume of 0.00181 km^3. (c) $M_{ej}(v > v_{esc})$ as a function of cohesion (Y_0) for the DART impact into targets with $f = 0.4$ and 0.55. (d) $M_{ej}(v > v_{esc})$ as a function of cohesion (Y_0) for the DART impact into targets with $f = 0.4$ and 0.55.

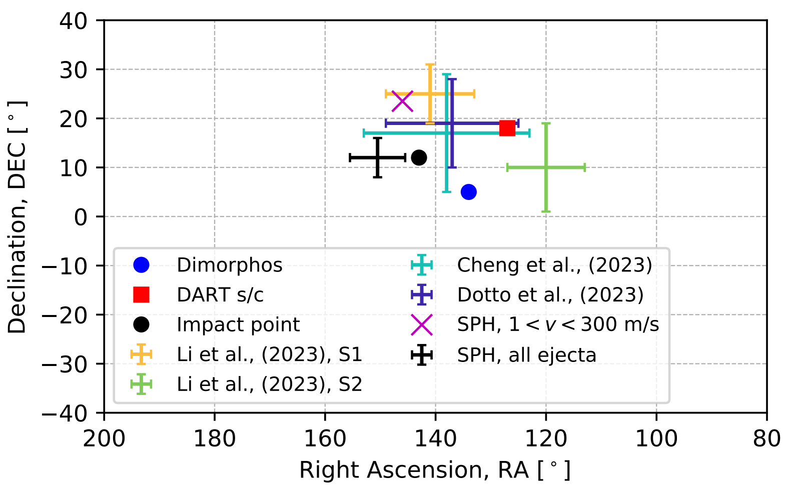

Supplementary Fig. 10: Ejecta cone orientation as derived from the HST data [141±8°, 25±6°; 120±9°, 10±7° Li2023], the LICIACube data [137±9°, 19±12° Dotto2023] and both [138±15°, +13±15° Cheng2023], compared to cone orientation derived from SPH simulations for ejecta with velocities between 1 and 300 m/s and for the entire range of ejecta [150.5±4°, 12±5°; 1-σ uncertainty]. The blue dot shows Dimorphos's velocity vector [134°,+5°], the red square is the direction of the incoming DART trajectory [128°,+18°] and the black dot shows the impact point at [143°,+12°].